Macromolecules

Article

pubs.acs.org/Macromolecules

Molecular Design and Application of a Photovoltaic Polymer with Improved Optical Properties and Molecular Energy Levels

Huifeng Yao, Hao Zhang, Long Ye, Wenchao Zhao, Shaoqing Zhang, and Jianhui Hou*

Beijing National Laboratory for Molecular Sciences, State Key Laboratory of Polymer Physics and Chemistry, Institute of Chemistry, Chinese Academy of Sciences, Beijing 100190, China

Supporting Information

ABSTRACT: (*E*)-5-(2-(5-(Alkylthio)thiophen-2-yl)vinyl)-thiophene-2-yl functional groups were introduced onto 4- and 8-positions of BDT units, and this building block was used to construct a new derivative polymer of PTB7, named as PBT-TVT. Benefiting from the prolonged conjugation of the conjugated side groups on BDT units, the optical absorption property of PBT-TVT can be improved greatly compared to that of PTB7, so an inspiring result of 7.67% was obtained by using PBT-TVT as the donor and $PC_{61}BM$ as the acceptor in polymer solar cells (PSCs), which is much higher than that of the PTB7:$PC_{61}BM$-based device and also one of the highest results for PSCs with $PC_{61}BM$. In electrochemical cyclic voltammetry (CV) measurements, PBT-TVT showed a deeper HOMO level than PTB7 so the device based on the former exhibits higher open circuit voltage than the latter. Moreover, in comparison with PTB7, the new polymer PBT-TVT exhibited stronger interchain $\pi-\pi$ interaction and thus higher hole mobility. Overall, the results in this work indicated that PBT-TVT is a promising donor polymer, and the strategy used in this work will be beneficial for molecular design of polymer photovoltaic materials for large-scale production of PSCs.

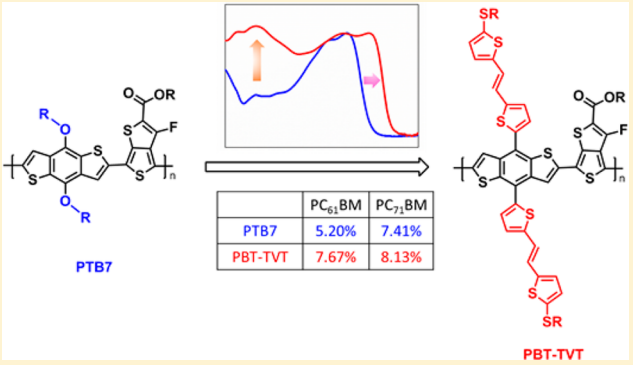

	$PC_{61}BM$	$PC_{71}BM$
PTB7	5.20%	7.41%
PBT-TVT	7.67%	8.13%

INTRODUCTION

PSC with bulk heterojunction structure (BHJ) has attracted considerable attention due to their potential in making large area and flexible solar panels by roll-to-roll printing process.[1−3] As is well-known, photovoltaic performance of PSCs is highly dependent on the properties of conjugated polymers that are used in their BHJ active layers, so tremendous efforts have been devoted to molecular design of conjugated polymers for the applications in PSCs and rapid progress has been achieved in the past decades.[4−11] By applying conjugated polymers with optimized molecular structures, the PCEs of single junction PSCs have been boosted to 10%.[12−16]

In order to realize high photovoltaic performance, the intrinsic properties of conjugated polymers, including their absorption spectra, molecular energy levels, hole mobilities, and morphologies, must be carefully tuned. First, conjugated polymers with broad absorption spectra and strong extinction coefficients are helpful to harvest the sunlight more efficiently, and thus the low band gap (LBG) polymers have been widely used and showed their superiorities of realizing high short circuit current density (J_{sc}) in PSCs. Since the open circuit voltage (V_{oc}) of PSCs is directly proportional to the gap between the HOMO of donor material and the LUMO of the acceptor material, conjugated polymers with deep HOMO levels have been employed to get high V_{oc}.[9,17−20] Moreover, from the point of view of facilitating the transport of carriers, conjugated polymers with strong interchain $\pi-\pi$ interaction, and thus better hole mobilities have been designed and applied. Overall, although quite a few new conjugated polymers have exhibited excellent photovoltaic properties,[12,13,21−26] to develop new methods that can improve all these above parameters in one conjugated polymer is still an important topic in the field of PSCs.

LBG polymers based on benzodithiophene (BDT)[4,27,28] and thienothiophene (TT)[29] units (PBDT-TTs) showed quite good photovoltaic properties so that these types of polymers have been studied extensively in the past a few years. PTB7[22,30,31] is a well-studied material in the family of PBDT-TTs. This polymer has a small optical band gap (E_g^{opt}) at about 1.6 eV and a rather good HOMO level at ca. −5.15 eV,[22] and also it possesses a comparatively broad optical absorption peak ranging from 550 to 750 nm. Moreover, although the crystallinity of PTB7 in solid film is not strong, it still can give a hole mobility of 5.8×10^{-4} $cm^2/(V\ s)$. Therefore, in PTB7-based PSCs with the conventional device architecture, i.e., using PEDOT:PSS as the p-type buffer layer and low work function metal as the cathode, the PCEs around 7−8% can be reproduced by many research groups.[31−34] Recently, a few research groups successfully applied inverted device configuration in PTB7-based PSCs and further promoted the PCEs to

Received: March 28, 2015
Revised: April 29, 2015
Published: May 19, 2015

DOI: 10.1021/acs.macromol.5b00649
Macromolecules 2015, 48, 3493−3499

Scheme 1. Molecular Structure and Synthetic Procedures of PBT-TVT

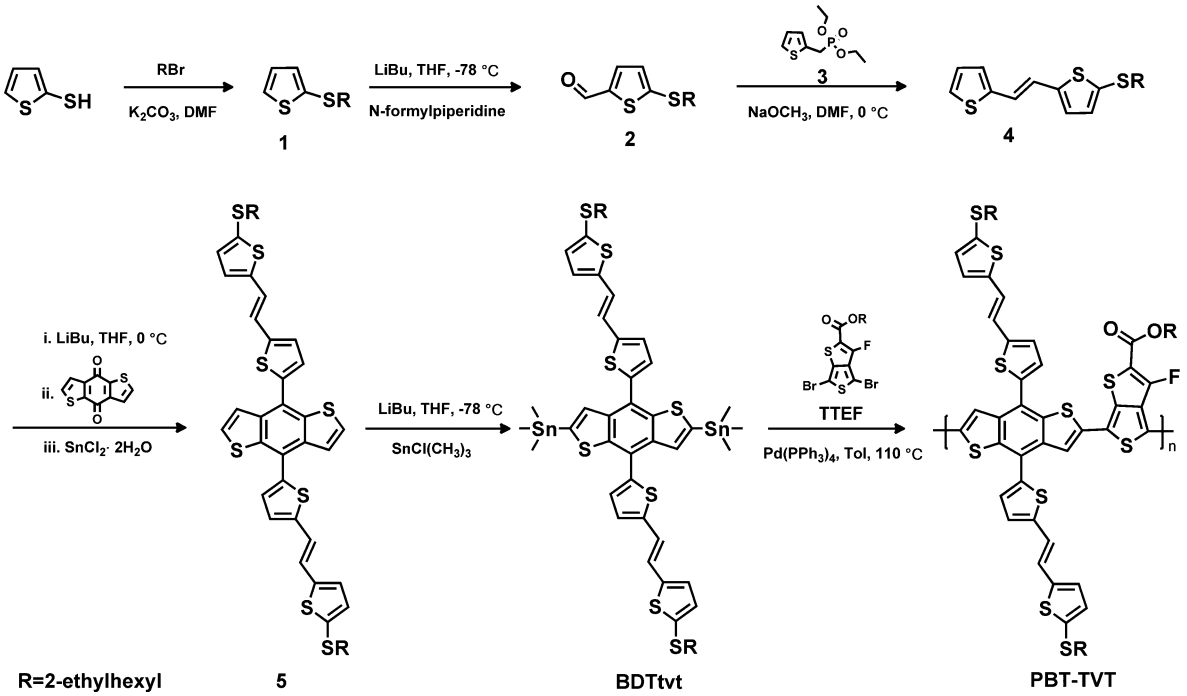

over 9%.[31,35,36] However, if we look back to the reported results of this polymer, we can find that the intrinsic properties of this polymer still need to be optimized. For example, the absorption spectrum of PTB7 is quite weak at the short wavelength range (300−550 nm), so $PC_{71}BM$, which has complementary absorption at short wavelength range with PTB7 but much higher cost than $PC_{61}BM$, must be used in the PTB7-based PSCs to harvest the sunlight more efficiently; the V_{oc} of PTB7-based device is limited to ca. 0.74 V due to the comparatively high HOMO level of the polymer;[22] the interchain $\pi-\pi$ interaction in PTB7 film is not strong so the hole mobility of PTB7 is not as high as the electron mobility of $PC_{71}BM$ or $PC_{61}BM$.[37,38] Therefore, if we can optimize the molecular structure of PTB7 and thus overcome these drawbacks, it can be expected that photovoltaic properties of this polymer will be improved, and also we can suggest a feasible path to optimize molecular structures of other types LBG polymers with similar properties as PTB7.

In this work, (*E*)-5-(2-(5-(alkylthio)thiophen-2-yl)vinyl)-thiophene-2-yl functional groups were introduced onto 4- and 8-positions of BDT units, and this building block was used to construct a new derivative polymer of PTB7, named as PBT-TVT. Benefiting from the prolonged conjugation of the conjugated side groups on BDT units, the optical absorption property of PBT-TVT can be improved greatly compared to that of PTB7, and also the new polymer shows a deeper HOMO level than PTB7. Moreover, in comparison with PTB7, the new polymer PBT-TVT exhibited stronger interchain $\pi-\pi$ interaction and thus higher hole mobility. As a result, the PSCs based on the new polymer demonstrated better photovoltaic performance than the device of PBT7, i.e., the V_{oc}, J_{sc}, and the overall PCE of the device of PBT-TVT prepared under the optimal condition are higher than those of the device of PTB7. More importantly, as reported for PTB7-based devices, when the acceptor material in the BHJ active layers was changed from $PC_{71}BM$ to $PC_{61}BM$, the PCE of the devices dropped from 7.4% to 4.4%;[39] however, for PBT-TVT-based devices, when $PC_{61}BM$ was used as the acceptor, a PCE of 7.67% still can be realized, which is similar as that of obtained from the device using $PC_{71}BM$ as the acceptor, so it can be concluded that the photovoltaic performance of the PBT-TVT-based devices were not sensitive to the absorption properties of the acceptor materials.

RESULTS AND DISCUSSION

Synthesis. The synthetic route of the new polymer is described in Scheme 1. The conjugated side chain of (*E*)-2-((2-ethylhexyl)thio)-5-(2-(thiophen-2-yl)vinyl)thiophene (compound **4**) was obtained by Knoevenagel reaction between 5-((2-ethylhexyl)thio)thiophene-2-carbaldehyde (compound **2**) and diethyl (thiophen-2-ylmethyl)phosphonate (compound **3**). Then the side chain was introduced onto BDT unit, and the monomer of BDTtvt was synthesized from the reaction with butyllithium and trimethyltin chloride. The preparation of the PBT-TVT was carried out through Stille coupling reaction between the monomers of BDTtvt and TTEF (as shown in Scheme 1). More synthetic details are given in the Experimental Section. The number-average molecular weight (M_n) of polymer is 19.5 kDa with a polydispersity index (PDI) of 6.25, estimated by gel permeation chromatography (GPC) using trichlorobenzene at 140 °C. Thermal stability of the polymer was evaluated by thermogravimetric analysis (TGA), and the plot is shown in Figure 1, from which it can be seen that the decomposition temperatures (T_d) at 5% weight loss is about 338 °C.

Optical Properties. The UV−vis absorption spectra of the solutions of the BDTtvt monomer and PBT-TVT in chlorobenzene are shown in Figure 2a, and the detailed parameters are listed in Table 1, and in order to make clear comparison with PTB7, the absorption spectrum and the corresponding parameters are also provided. The monomer gives an absorption peak at ca. 432 nm, and this absorption feature can be kept in polymer but is slightly blue-shifted to 396

DOI: 10.1021/acs.macromol.5b00649
Macromolecules 2015, 48, 3493−3499

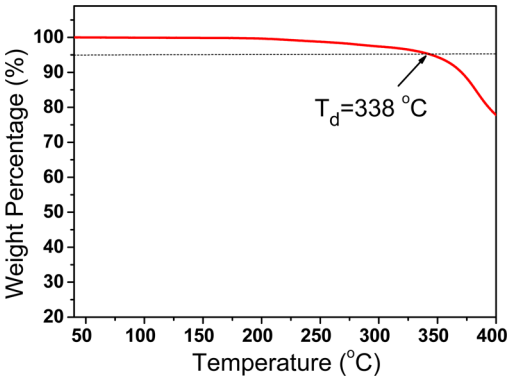

Figure 1. TGA plot of PBT-TVT under the protection of nitrogen with a heating rate of 10 °C/min.

nm, and this phenomenon is similar to that reported works related two two-dimensional conjugated polythiophenes.[40−42] In comparison with PTB7, the polymer PBT-TVT exhibits a much broader absorption spectrum; i.e., the absorption edge of PBT-TVT is at ca. 810 nm, which is 60 nm red-shifted than that of PTB7 and the absorption of PBT-TVT is also much stronger than that of PTB7 in the range from 300 to 600 nm.

The optical densities of the PBT-TVT and PTB7 films with 100 nm thickness are provided in Figure 2b. It is shown that the peak value of the PBT-TVT film is quite similar to that of PTB7; i.e., the extinction coefficients of PBT-TVT and PTB7 are 9.38×10^4 cm^{-1} and 9.40×10^4 cm^{-1} (see Figure S1), respectively. It is clear that the absorption spectrum of the PBT-TVT film covers the whole range from 300 to 810 nm, and also in the whole range, the optical density of the PBT-TVT is quite high. From the aspect of absorption properties, for the PSCs based on PBT-TVT, panchromatic absorption can be realized without using another absorber with complementary absorption. Therefore, the broad and strong absorption spectrum of PBT-TVT makes it to be an excellent light absorber in PSCs.

Electrochemical Properties. The HOMO of PBT-TVT was measured by electrochemical cyclic voltammetry (CV). As shown in Figure 3, the CV plots of p-doping process of PBT-TVT and PTB7 are provided in parallel, and they were measured on glassy carbon working electrode in 0.1 M Bu_4NPF_6 acetonitrile solution at a scan rate of 20 mV/s. The onset oxidation potentials (ϕ_{ox}) of PBT-TVT and PTB7 are 0.49 and 0.43 V, corresponding to HOMO levels of −5.29 and −5.23 eV, respectively. These results indicate that the HOMO level of PTB7 can be reduced by replacing alkoxy with (*E*)-2-((2-ethylhexyl)thio)-5-(2-(thiophen-2-yl)vinyl)thiophene, which will be helpful to realize higher V_{oc} in device.

Table 1. Optical and Electrochemical Properties of the Polymer Films

polymer	λ_{onset} (nm)	E_g^{opt} (eV)	HOMO (eV)	λ_{max} (nm)/ ε (10^4 cm^{-1})	μ_{hole} ($cm^2/(V\ s)$)
PBT-TVT	810	1.53	−5.29	402 (9.40), 665 (9.34), 734 (9.38)	9.54×10^{-4}
PTB7	760	1.63	−5.23	626 (8.31), 676 (9.16)	4.28×10^{-4}

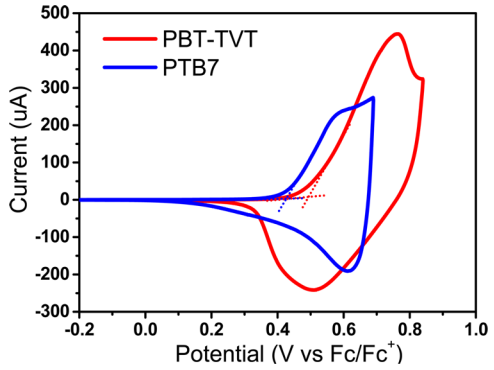

Figure 3. Cyclic voltammograms of the PBT-TVT and PTB7 film on the glassy carbon electrode in 0.1 M Bu_4NPF_6 acetonitrile solution at a scan rate of 20 mV/s.

Theoretical Calculation. Theoretical calculation was performed to predict the electronic properties and energy levels of the polymer by using the density functional theory (DFT) with the B3LYP/6-31G** basis set (Gaussian 09).[43] In order to reduce the cost of calculation, the long alkyl chains were replaced by CH_3 groups, and the polymer was simplified to dimer. The optimized molecular geometries and frontier molecular orbitals are illustrated in Figure 4. For PTB7, the HOMO and LUMO surfaces are well delocalized along its backbone. However, for PBT-TVT, although the LUMO surface is mainly localized on the backbone of the main chain and partially delocalized on the conjugated side groups, the HOMO surface can be delocalized along the whole conjugated backbone. Apparently, for PBT-TVT, the side groups are well conjugated with the main chain, so more π-electrons can make contribution to the absorption spectrum; on the other hand, this feature extends the conjugation area of the polymer, which is benefit for improving interchain $\pi-\pi$ interaction, so PBT-TVT may possess higher hole mobility than PTB7. In addition,

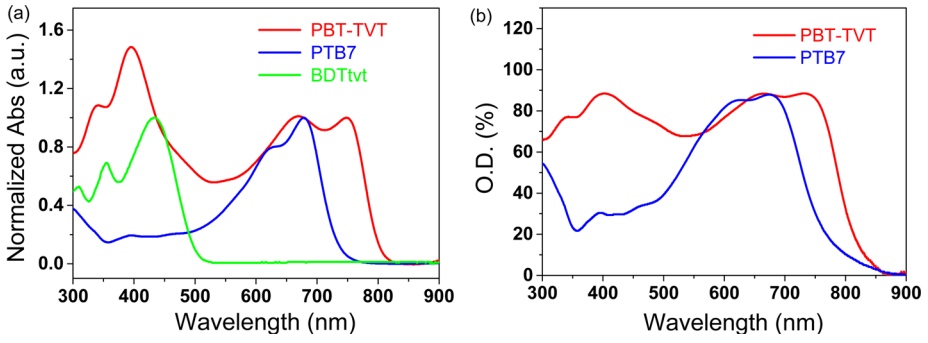

Figure 2. Absorption spectra of the polymers: (a) normalized absorption spectra of compound BDTtvt and the polymers in chlorobenzene solution and (b) optical density of 100 nm thickness films of the polymers.

DOI: 10.1021/acs.macromol.5b00649
Macromolecules 2015, 48, 3493−3499

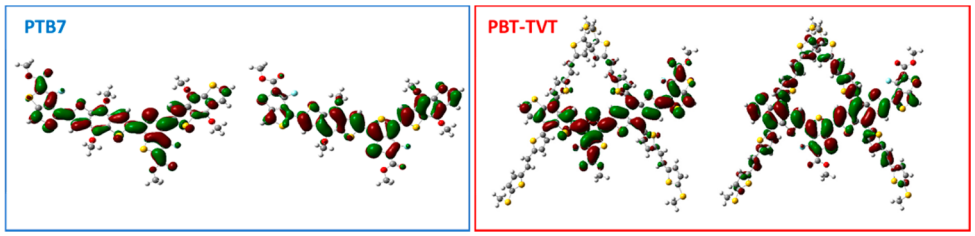

Figure 4. Simulated HOMO (right) and LUMO (left) electron density distributions of the two polymers by DFT with the B3LYP/6-31G** basis set.

the calculated HOMO levels of PTB7 and PBT-TVT are similar, ca. −5.0 eV, for the simplified model used in the calculation.

X-ray Diffraction Analysis. The crystalline properties of PBT-TVT and PTB7 were investigated by X-ray diffraction (XRD) measurement. As shown in Figure 5, no clear lamellar

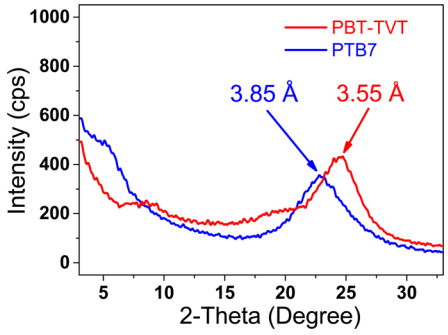

Figure 5. XRD patterns of PBT-TVT and PTB7 films coated from chlorobenzene onto a silicon substrate.

diffraction signal can be observed for both two films of PBT-TVT and PTB7, suggesting that there are barely ordered arrangement in the films of the two polymers toward lamellar direction. In contrast, the features of $\pi-\pi$ stacking can be observed in both PBT-TVT and PTB7. The diffraction peak of the PTB7 film appeared at $2\theta = 22.79°$, corresponding to a $\pi-\pi$ distance of 3.85 Å, which is coincident with the reported work.[44] The film of PBT-TVT showed a stronger refection signal at $2\theta = 24.72°$, corresponding to a $\pi-\pi$ stacking distance of 3.55 Å, which is much smaller than that of PTB7 film and also is one of the smallest values for conjugated polymers.[45] As known, compact $\pi-\pi$ stack are helpful to facilitate the interchain π-electron transport in conjugated polymers,[4] so it can be expected that PBT-TVT may possess high hole mobility than PTB7. Consequently, the space-charge-limited current (SCLC) method[46] was used to evaluate the hole mobilities of these two polymers. Herein, a hole only device with a configuration of ITO/PEDOT:PSS/polymer/Au was employed, and the corresponding curves are provided in Figure S2 (see Supporting Information). The hole mobility of the PBT-TVT was calculated to be 9.54×10^{-4} cm^2/(V s), which is higher than that of PTB7 (ca. 4.28×10^{-4} cm^2/(V s) in this work and 5.8×10^{-4} cm^2/(V s) in reported work[22]). Therefore, the data obtained from the XRD analysis and SCLC measurements indicate that the replacement of alkoxyl by the functional group of (*E*)-5-(2-(5-(alkylthio)thiophen-2-yl)-vinyl)thiophene-2-yl can induce stronger interchain $\pi-\pi$ interaction and thus facilitate hole transport.

Photovoltaic Characterizations. Photovoltaic properties of PBT-TVT were evaluated and compared with that of PTB7 by employing a conventional device structure of ITO/PEDOT:PSS/polymer:fullerene/Mg/Al, in which $PC_{71}BM$ was initially used as the acceptor material. Herein, for making the control device based on PTB7, the optimized device fabrication process as demonstrated in reported works[22] was followed. Since PBT-TVT is a new polymer, the device fabrication process was optimized as follow. First, different polymer:$PC_{71}BM$ (D/A) weight ratios were scanned by using chlorobenzene (CB) as solvent. As shown in Table S1, the optimal D/A ratio is 1:1.5. Then, varied amounts of 1,8-diiodoctane (DIO) were scanned to further optimize photovoltaic performance of the devices, and we found that the best PCE was obtained by using 7% volume ratio of DIO (see Table S2).

The PSCs devices based on PBT-TVT:$PC_{71}BM$ and PTB7:$PC_{71}BM$ were prepared and characterized in parallel to make clear comparisons. The current density and voltage (*J*−*V*)

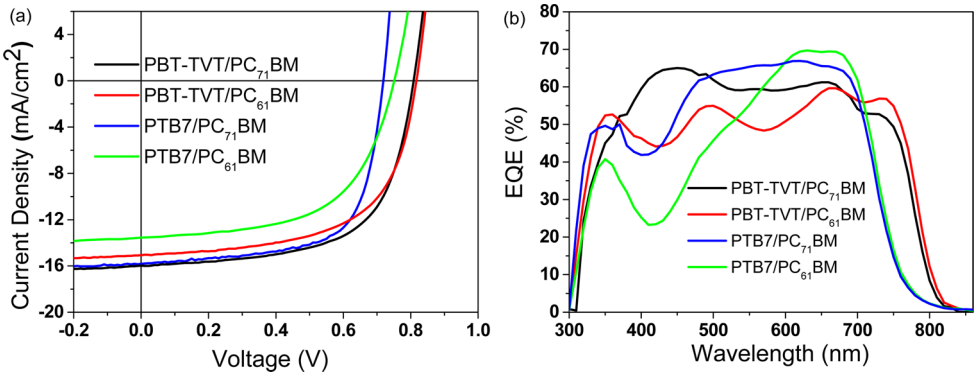

Figure 6. (a) *J*−*V* curves of the PSC devices under illumination of AM 1.5G (100 mW/cm^2). (b) External quantum efficiency (EQE) curves of the corresponding devices.

DOI: 10.1021/acs.macromol.5b00649
Macromolecules 2015, 48, 3493−3499

curves of the corresponding devices are as shown in Figure 6a, and the photovoltaic parameters are listed in Table 2. The

Table 2. Photovoltaic Parameters of Devices Based on the Two Polymers Blend with the Fullerene Acceptors

	V_{oc} (V)	J_{sc}[b] (mA/cm^2)	FF (%)	PCE[c] (%)
PBT-TVT:$PC_{71}BM$	0.81	16.00 (15.16)	62.71	8.13 (8.04)
PTB7:$PC_{71}BM$	0.73	15.74 (14.73)	64.36	7.41 (7.39)
PTB7:$PC_{71}BM$[a22]	0.74	14.50	68.97	7.4
PBT-TVT:$PC_{61}BM$	0.82	14.64 (13.94)	63.92	7.67 (7.50)
PTB7:$PC_{61}BM$	0.75	11.08 (11.06)	62.52	5.20 (5.16)
PTB7:$PC_{61}BM$[a39]	0.74	10.9	54.8	4.4

[a]These data are obtained from the corresponding reference as noted. [b]Calculated J_{sc} from EQE calculated by integrating the EQE spectrum was shown in the parentheses. [c]The value in the parentheses is the average PCE obtained from 10 devices.

PTB7:$PC_{71}BM$-based device showed a PCE of 7.41% with a V_{oc} of 0.73 V and a J_{sc} of 15.74 mA/cm^2, and these data are very similar to the reported works.[22] For PBT-TVT:$PC_{71}BM$-based device, the V_{oc} reached 0.81 V, which is 0.08 V higher than that of the device of PTB7:$PC_{71}BM$. In EQE measurements (see Figure 6b), the PBT-TVT:$PC_{71}BM$-based device exhibits a much broader response range than the PTB7:$PC_{71}BM$-based device; therefore, although the quantum efficiency of the former is slightly lower than the latter in the range of 500−700 nm, the former device still exhibited a higher J_{sc} than the latter. Overall, the PCE of PBT-TVT:$PC_{71}BM$-devcie reached 8.13%, which is obviously higher than that of the device of PTB7:$PC_{71}BM$.

As well-known, $PC_{71}BM$ is often used in the PSCs based on LBG polymers due to its complementary absorption property. For PTB7-based devices, when the acceptor was changed from $PC_{71}BM$ to $PC_{61}BM$, the J_{sc} dropped from 14.5 to 10.9 mA/cm^2.[39] In this work, we reproduced the above experiments and observed very similar phenomena. As mentioned previously, for the pure film of PBT-TVT, panchromatic absorption can be easily realized, so the device based on PBT-TVT:$PC_{61}BM$ was prepared to utilize this unique property of this polymer. As shown in Figure 6a, the PBT-TVT:$PC_{61}BM$-based device prepared under the optimal condition (the optimization processing are shown in Supporting Information, Tables S3 and S4) exhibits a panchromatic photoresponse for the sunlight and thus a relatively high J_{sc} of 14.64 mA/cm^2. Therefore, a desirable PCE of 7.67% was recorded in the PBT-TVT:$PC_{61}BM$ device, which is much higher than that of the PTB7:$PC_{61}BM$-based device.

Morphology Study. Atomic force microscopy (AFM) and transmission electron microscopy (TEM) were used to gain insight into the morphology of the blend films coated by the polymers and fullerene acceptor. As depicted in Figure 7a,b,d,e, the blend films of PBT-TVT:$PC_{61}BM$ and PTB7:$PC_{61}BM$ showed very similar morphological properties in AFM measurements, i.e., the mean-square surface roughness (R_q) of PBT-TVT:$PC_{61}BM$ is 0.92 nm, which was slightly smaller than PTB7:$PC_{61}BM$ (1.03 nm), and the aggregation size and features observed in the phase images for these two blend films are also very similar. The TEM images of the blend films are exhibited in Figure 7c,f, and both of them show uniform morphologies and appropriate domain sizes, which are similar to the results observed from the PTB7:$PC_{71}BM$.[22] The favorable morphology gained from the blend film based on PBT-TVT suggested that the introduction of long conjugated side chain would not change the miscibility of the polymer and fullerene acceptor.

Conclusion. In conclusion, a novel photovoltaic polymer derived from PTB7 with prolonged conjugated side chain, (*E*)-2-((2-ethylhexyl)thio)-5-(2-(thiophen-2-yl)vinyl)thiophene, was designed and synthesized. Compared to PTB7, the absorption spectrum of PBT-TVT extended to 810 nm, and the new polymer had a lower HOMO level (−5.29 eV). Furthermore, XRD analysis suggested a closer interchain $\pi-\pi$ stacking (3.55 Å) existed in PBT-TVT film than that of PTB7. When $PC_{71}BM$ was used as the acceptor in the active layer, the PSC devices exhibited a high PCE of 8.13% with a V_{oc} of 0.81 V. More importantly, due to its panchromatic absorption of PBT-TVT, an inspiring results of 7.67% was obtained by using low-cost $PC_{61}BM$[47] as acceptor in BHJ devices, which is one of the highest results for PSCs based on $PC_{61}BM$. AFM and TEM

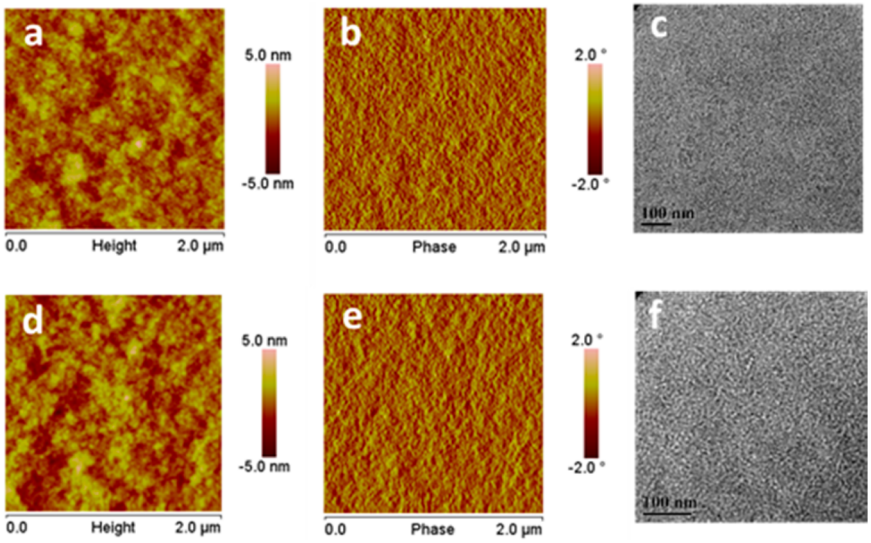

Figure 7. Morphology images of polymers:$PC_{61}BM$ films: (a) AFM height images, (b) phase images, and (c) TEM images of PTB7:$PC_{61}BM$ and (d) AFM height images, (e) phase images (f), and TEM images of PBT-TVT:$PC_{61}BM$.

DOI: 10.1021/acs.macromol.5b00649
Macromolecules 2015, 48, 3493−3499

results suggested that the introducing of long conjugated side chain would not change the morphology of mixture very much. All the results indicated that PBT-TVT is a promising donor polymer, and the molecular design strategy used in this work will be beneficial for molecular design of polymer photovoltaic materials for large-scale production of PSCs.

EXPERIMENTAL SECTION

Materials and Synthesis. Diethyl (thiophen-2-ylmethyl)-phosphonate, benzo[1,2-*b*:4,5-*b*′]dithiophene-4,8-dione, PTB7, $PC_{61}BM$, and $PC_{71}BM$ were commercially available from Solarmer Material Inc. The monomer of TTEF was purchased from Suna Tech Inc. $Pd(PPh_3)_4$ was purchased from Frontiers Scientific Inc. Tetrahydrofuran (THF) was dried over Na/benzophenone and freshly distilled prior to use. The other materials were common commercial level and used as received.

*2-(2-Ethylhexylthio)thiophene (**1**).* To a solution of thiophene-2-thiol (11.6 g, 0.1 mol) and K_2CO_3 (20.7 g, 0.15 mol) in DMF (100 mL), 1-bromo-2-ethylhexane (19.3 g, 0.1 mol) was added. The reaction mixture was stirred at 80 °C for 4 h. After cooling to ambient temperature, the mixture was filtered, and the residue was poured into cool water and extracted by diethyl ether three times. After the solvent was removed, the crude product was purified by distillation, and 18.6 g of compound **1** (0.08 mol, yield 81%) was obtained. GC-MS: m/z = 228. ^{1}H NMR ($CDCl_3$, 400 MHz) spectrum is provided in Figure S3a.

*5-((2-Ethylhexyl)thio)thiophene-2-carbaldehyde (**2**).* Compound **1** (11.4 g, 50 mmol) was dissolved in anhydrous THF (150 mL) under an argon atmosphere; *n*-butyllithium (2.5 M, 22 mL) was added dropwise at −78 °C. After the mixture was stirred for 1 h, *N*-formylpiperidine (7.9 g, 70 mmol) was added in one portion. The reaction was quenched by water after 0.5 h, and then the mixture was extracted by diethyl ether three times. After the combined organic phase was concentrated, further purification was carried out by silica gel column chromatography with petroleum ether and ethyl acetate (30:1) as the eluent. The pure compound **2** was obtained as yellow oil (10 g, yield 78%). ^{1}H NMR ($CDCl_3$, 400 MHz) spectrum is provided in Figure S3b.

*(E)-2-((2-Ethylhexyl)thio)-5-(2-(thiophen-2-yl)vinyl)thiophene (**4**).* Compound **2** (5.1 g, 20 mmol) was added to a solution of diethyl (thiophen-2-ylmethyl)phosphonate (compound **3**) (4.7 g, 20 mmol) and sodium methylate (1.2 g, 22 mmol) in DMF (20 mL) at 0 °C. After 1 h of stirring, the reaction was quenched by water and extracted by ethyl acetate. The solvent was removed via rotary evaporation, and then the crude product was purified by silica gel column chromatography with petroleum ether as eluent. Compound **3** (5.1 g, yield 76%) was obtained as sticky yellow oil. ^{1}H NMR (acetone-*d*, 400 MHz) spectrum is provided in Figure S3c.

*4,8-Bis(5-((E)-2-(5-((2-ethylhexyl)thio)thiophen-2-yl)vinyl)-thiophen-2-yl)benzo[1,2-b:4,5-b′]dithiophene (**5**).* *n*-Butyllithium (2.5 M, 4 mL) was added dropwise into a solution of compound **3** (3 g, 9 mmol) in THF (15 mL) at 0 °C under protection of argon, and then the mixture was warmed to 50 °C and stirred for 0.5 h. Subsequently, benzo[1,2-*b*:4,5-*b*′]dithiophene-4,8-dione (0.66 g, 3 mmol) was injected in the flask and stirred for 1 h, and then a solution of $SnCl_2{\cdot}2H_2O$ (4.7 g, 21 mmol) in 10% HCl was added at room temperature and stirred for another 2 h. After the mixture was extracted by water and diethyl ether, the organic phase was concentrated by removing of solvent, and the raw product was purified by silica gel chromatography to get pure compound **5** as reddish-yellow solid (1.8 g, yield 70%). ^{1}H NMR ($CDCl_3$, 400 MHz) spectrum is provided in Figure S3d.

(4,8-Bis(5-((E)-2-(5-((2-ethylhexyl)thio)thiophen-2-yl)vinyl)-thiophen-2-yl)benzo[1,2-b:4,5-b′]dithiophene-2,6-diyl)bis-(trimethylstannane) (BDTtvt). Under protection of argon, *n*-butyllithium (2.5 M, 2 mL) was added dropwise into a solution of compound **5** (1.7 g, 2 mmol) in THF (15 mL) at −78 °C. After 0.5 h of reaction, trimethyltin chloride solution (1.0 M in THF, 6 mL) was added and stirred for 10 min, and then the cooling bath was removed and stirred for another 1 h at ambient temperature. The mixture was poured into water and extracted by ether, and the organic layer was concentrated to obtain the crude compound **M1**. Acetone was used to recrystallize for further purification, after which the pure BDTtvt (1.5 g, yield 64%) was obtained as yellow solid. ^{1}H NMR and ^{13}C NMR ($CDCl_3$, 400 MHz) spectra are provided in Figures S3e and S3f. Anal. Calcd for $C_{52}H_{66}S_8Sn_2$: C, 52.70; H, 5.61. Found: C, 52.62; H, 5.62.

Synthesis of the Polymer PBT-TVT by Stille Coupling. 0.3 mmol of BDTtvt and an equal quantity of TTEF were dissolve in toluene (8 mL) and DMF (1.5 mL); after being flushed with argon for 5 min, $Pd(PPh_3)_4$ (17 mg) was added. Then the mixture was purged with argon for another 15 min, after which the reaction mixture was stirred at 110 °C for 4 h. When the mixture was cooled to ambient temperature, the polymer was precipitated by addition of methanol (80 mL). The precipitates was purified by Soxhlet extraction with methanol, hexanes, and chloroform. The polymer was recovered from chloroform fraction by precipitation from methanol. The solid (yield 49%) was dried under vacuum for 24 h. ^{1}H NMR ($CDCl_3$, 400 MHz) spectrum is provided in Figure S3g. Elemental analysis calcd (%) for $C_{61}H_{67}FO_2S_{10}$: C 62.52, H 5.76. Found: C 61.69, H 5.68.

Instruments and Measurements. ^{1}H NMR and ^{13}C NMR spectra were taken on a Bruker AVANCE 400 MHz spectrometer at room temperature to confirm the structures of the compounds. Elemental analysis was conducted on a flash EA1112 analyzer. Absorption spectra of polymers in solution and solid thin films were measured on a Hitachi U-3100 UV−vis spectrophotometer. Molecular weight and polydispersity (PDI) of the polymer were obtained by gel permeation chromatography (GPC) using 1,2,4-trichlorobenzene as eluent at 140 °C. The CV measurements were conducted on a CHI650D electrochemical workstation with glassy carbon, platinum wire, and Ag/Ag^+ electrode as working electrode, counter electrode, and reference electrode, respectively, in a 0.1 M tetrabutylammonium hexafluorophosphate (Bu_4NPF_6)−acetonitrile solution. In order to obtain reliable results, $J-V$ characteristics were measured under 100 mW/cm^2 standard AM 1.5 G spectrum by using a Class AAA solar simulator along with a NIM calibrated KG3-filtered reference cells following our recent report.[48] The EQE was measured by an integrated IPCE system named QE-R3011 (Enli Technology Co. Ltd., Taiwan). The AFM images were obtained by a Nanoscope V AFM on tapping mode, and TEM images were performed on a JEOL 2200FS instrument at 160 kV accelerating voltage in bright-field mode.

Fabrication of the PSC Devices. All the devices have the same structure of ITO/PEDOT:PSS/polymer:acceptor/Mg (20 nm)/Al (80 nm) and fabricated under the following conditions: the purchased ITO glasses were cleaned by a surfactant scrub and washed by water, acetone, and isopropanol, successively. After 15 min of UV-ozone treating, about 35 nm thick of PEDOT:PSS was spin-coated on the ITO glasses. Then the ITO substrate were dried in an oven at 150 °C for 15 min. Blend solutions of PBT-TVT:$PC_{61}BM$ or PBT-TVT:$PC_{71}BM$ (10 mg/mL, based on polymer weight concentration, with or without DIO) were spin-coated on PEDOT:PSS layer. The devices based on PTB7:$PC_{71}BM$ and PTB7:$PC_{61}BM$ were prepared according to reported works. After the active layer was spin-coated on the PEDOT:PSS, a small amount of methanol was spin-coated on it at 4000 rpm for 30 s to remove the residual additives.[49] Finally, about 20 nm of Mg and 80 nm of Al with an area of 4.15 mm^2 were deposited onto the active layer under high vacuum successively. All the processes except for the spin-coating of PEDOT:PSS were carried out in a glovebox of nitrogen atmosphere.

ASSOCIATED CONTENT

Supporting Information

Absorption coefficient of the polymer films, hole mobility measurement, and the details of optimization of PSC devices. The Supporting Information is available free of charge on the ACS Publications website at DOI: 10.1021/acs.macromol.5b00649.

DOI: 10.1021/acs.macromol.5b00649
Macromolecules 2015, 48, 3493−3499

AUTHOR INFORMATION

Corresponding Author

*(J.H.) E-mail: hjhzlz@iccas.ac.cn.

Notes

The authors declare no competing financial interest.

ACKNOWLEDGMENTS

The authors acknowledge the financial support from Ministry of Science and Technology of China (No. 2014CB643501), NSFC (Nos. 21325419, 91333204), and the Chinese Academy of Science (Nos. XDB12030200, KJZD-EW-J01).

REFERENCES

(1) Yu, G.; Gao, J.; Hummelen, J. C.; Wudl, F.; Heeger, A. J. *Science* **1995**, *270*, 1789−1791.
(2) Heeger, A. J. *Adv. Mater.* **2014**, *26*, 10−27.
(3) Li, G.; Zhu, R.; Yang, Y. *Nat. Photonics* **2012**, *6*, 153−161.
(4) Ye, L.; Zhang, S.; Huo, L.; Zhang, M.; Hou, J. *Acc. Chem. Res.* **2014**, *47*, 1595−1603.
(5) Li, Y. F. *Acc. Chem. Res.* **2012**, *45*, 723−733.
(6) Henson, Z. B.; Mullen, K.; Bazan, G. C. *Nat. Chem.* **2012**, *4*, 699−704.
(7) Duan, C.; Huang, F.; Cao, Y. *J. Mater. Chem.* **2012**, *22*, 10416−10434.
(8) Beaujuge, P. M.; Fréchet, J. M. J. *J. Am. Chem. Soc.* **2011**, *133*, 20009−20029.
(9) Zhang, H.; Ye, L.; Hou, J. *Polym. Int.* **2015**, DOI: 10.1002/pi.4895.
(10) Kang, T. E.; Kim, K.-H.; Kim, B. J. *J. Mater. Chem. A* **2014**, *2*, 15252−15267.
(11) Kang, T. E.; Cho, H.-H.; Kim, H. j.; Lee, W.; Kang, H.; Kim, B. J. *Macromolecules* **2013**, *46*, 6806−6813.
(12) Zhang, S.; Ye, L.; Zhao, W.; Yang, B.; Wang, Q.; Hou, J. *Sci. China Chem.* **2015**, *58*, 248−256.
(13) Liu, Y.; Zhao, J.; Li, Z.; Mu, C.; Ma, W.; Hu, H.; Jiang, K.; Lin, H.; Ade, H.; Yan, H. *Nat. Commun.* **2014**, *5*, 5293.
(14) Chen, J. D.; Cui, C.; Li, Y. Q.; Zhou, L.; Ou, Q. D.; Li, C.; Li, Y.; Tang, J. X. *Adv. Mater.* **2015**, *27*, 1035−1041.
(15) He, Z.; Xiao, B.; Liu, F.; Wu, H.; Yang, Y.; Xiao, S.; Wang, C.; Russell, T. P.; Cao, Y. *Nat. Photonics* **2015**, *9*, 174−179.
(16) Liao, S. H.; Jhuo, H. J.; Yeh, P. N.; Cheng, Y. S.; Li, Y. L.; Lee, Y. H.; Sharma, S.; Chen, S. A. *Sci. Rep.* **2014**, *4*, 6813.
(17) Chen, H. Y.; Hou, J. H.; Zhang, S. Q.; Liang, Y. Y.; Yang, G. W.; Yang, Y.; Yu, L. P.; Wu, Y.; Li, G. *Nat. Photonics* **2009**, *3*, 649−653.
(18) Cui, C.; Wong, W.-Y.; Li, Y. *Energy Environ. Sci.* **2014**, *7*, 2276−2284.
(19) Ye, L.; Zhang, S.; Zhao, W.; Yao, H.; Hou, J. *Chem. Mater.* **2014**, *26*, 3603−3605.
(20) Yao, H.; Ye, L.; Fan, B.; Huo, L.; Hou, J. *Sci. China Mater.* **2015**, *58*, 213−222.
(21) Huo, L.; Zhang, S.; Guo, X.; Xu, F.; Li, Y.; Hou, J. *Angew. Chem.* **2011**, *50*, 9697−9702.
(22) Liang, Y.; Xu, Z.; Xia, J.; Tsai, S.-T.; Wu, Y.; Li, G.; Ray, C.; Yu, L. *Adv. Mater.* **2010**, *22*, E135−E138.
(23) Liao, S.-H.; Jhuo, H.-J.; Cheng, Y.-S.; Chen, S.-A. *Adv. Mater.* **2013**, *25*, 4766−4711.
(24) Zhang, M.; Gu, Y.; Guo, X.; Liu, F.; Zhang, S.; Huo, L.; Russell, T. P.; Hou, J. *Adv. Mater.* **2013**, *25*, 4944−4949.
(25) Cabanetos, C.; El Labban, A.; Bartelt, J. A.; Douglas, J. D.; Mateker, W. R.; Frechet, J. M. J.; McGehee, M. D.; Beaujuge, P. M. *J. Am. Chem. Soc.* **2013**, *135*, 4656−4659.
(26) Liu, P.; Zhang, K.; Liu, F.; Jin, Y.; Liu, S.; Russell, T. P.; Yip, H.-L.; Huang, F.; Cao, Y. *Chem. Mater.* **2014**, *26*, 3009−3017.
(27) Hou, J. H.; Park, M. H.; Zhang, S. Q.; Yao, Y.; Chen, L. M.; Li, J. H.; Yang, Y. *Macromolecules* **2008**, *41*, 6012−6018.
(28) Huo, L.; Hou, J. *Polym. Chem.* **2011**, *2*, 2453−2461.
(29) Liang, Y.; Feng, D.; Wu, Y.; Tsai, S.-T.; Li, G.; Ray, C.; Yu, L. *J. Am. Chem. Soc.* **2009**, *131*, 7792−7799.
(30) Lu, L.; Yu, L. *Adv. Mater.* **2014**, *26*, 4413−4430.
(31) He, Z.; Zhong, C.; Su, S.; Xu, M.; Wu, H.; Cao, Y. *Nat. Photonics* **2012**, *6*, 591−595.
(32) Zhou, H.; Zhang, Y.; Mai, C.-K.; Collins, S. D.; Nguyen, T.-Q.; Bazan, G. C.; Heeger, A. J. *Adv. Mater.* **2014**, *26*, 780−785.
(33) Zhao, W.; Ye, L.; Zhang, S.; Fan, B.; Sun, M.; Hou, J. *Sci. Rep.* **2014**, *4*, 6570.
(34) Baek, S.-W.; Noh, J.; Lee, C.-H.; Kim, B.; Seo, M.-K.; Lee, J.-Y. *Sci. Rep.* **2013**, *3*, 1726.
(35) Liu, S.; Zhang, K.; Lu, J.; Zhang, J.; Yip, H.-L.; Huang, F.; Cao, Y. *J. Am. Chem. Soc.* **2013**, *135*, 15326−15329.
(36) Zhang, W.; Wu, Y.; Bao, Q.; Gao, F.; Fang, J. *Adv. Energy Mater.* **2014**, *4*, 1400359.
(37) Ye, L.; Zhang, S. Q.; Qian, D. P.; Wang, Q.; Hou, J. H. *J. Phys. Chem. C* **2013**, *117*, 25360−25366.
(38) Foster, S.; Deledalle, F.; Mitani, A.; Kimura, T.; Kim, K. B.; Okachi, T.; Kirchartz, T.; Oguma, J.; Miyake, K.; Durrant, J. R.; Doi, S. J.; Nelson, J. *Adv. Energy Mater.* **2014**, *4*, 1400311.
(39) Chen, W.; Xu, T.; He, F.; Wang, W.; Wang, C.; Strzalka, J.; Liu, Y.; Wen, J.; Miller, D. J.; Chen, J.; Hong, K.; Yu, L.; Darling, S. B. *Nano Lett.* **2011**, *11*, 3707−3713.
(40) Chung, H.-S.; Lee, W.-H.; Song, C. E.; Shin, Y.; Kim, J.; Lee, S. K.; Shin, W. S.; Moon, S.-J.; Kang, I.-N. *Macromolecules* **2013**, *47*, 97−105.
(41) Hou, J.; Tan, Z. A.; He, Y.; Yang, C.; Li, Y. *Macromolecules* **2006**, *39*, 4657−4662.
(42) Lee, J.; Kim, J.-H.; Moon, B.; Kim, H. G.; Kim, M.; Shin, J.; Hwang, H.; Cho, K. *Macromolecules* **2015**, *48*, 1723−1735.
(43) Frisch, M. J.; Trucks, G. W.; Schlegel, H. B.; Scuseria, G. E.; Robb, M. A.; Cheeseman, J. R.; Scalmani, G.; Barone, V.; Mennucci, B.; Petersson, G. A.; Nakatsuji, H.; Caricato, M.; Li, X.; Hratchian, H. P.; Izmaylov, A. F.; Bloino, J.; Zheng, G.; Sonnenberg, J. L.; Hada, M.; Ehara, M.; Toyota, K.; Fukuda, R.; Hasegawa, J.; Ishida, M.; Nakajima, T.; Honda, Y.; Kitao, O.; Nakai, H.; Vreven, T.; Montgomery Jr., J. A.; Peralta, J. E.; Ogliaro, F.; Bearpark, M. J.; Heyd, J.; Brothers, E. N.; Kudin, K. N.; Staroverov, V. N.; Kobayashi, R.; Normand, J.; Raghavachari, K.; Rendell, A. P.; Burant, J. C.; Iyengar, S. S.; Tomasi, J.; Cossi, M.; Rega, N.; Millam, N. J.; Klene, M.; Knox, J. E.; Cross, J. B.; Bakken, V.; Adamo, C.; Jaramillo, J.; Gomperts, R.; Stratmann, R. E.; Yazyev, O.; Austin, A. J.; Cammi, R.; Pomelli, C.; Ochterski, J. W.; Martin, R. L.; Morokuma, K.; Zakrzewski, V. G.; Voth, G. A.; Salvador, P.; Dannenberg, J. J.; Dapprich, S.; Daniels, A. D.; Farkas, Ö.; Foresman, J. B.; Ortiz, J. V.; Cioslowski, J.; Fox, D. J. *Gaussian 09*; Gaussian, Inc.: Wallingford, CT, 2009.
(44) Liu, F.; Zhao, W.; Tumbleston, J. R.; Wang, C.; Gu, Y.; Wang, D.; Briseno, A. L.; Ade, H.; Russell, T. P. *Adv. Energy Mater.* **2014**, *4*, 1301377.
(45) Huang, Y.; Guo, X.; Liu, F.; Huo, L. J.; Chen, Y. N.; Russell, T. P.; Han, C. C.; Li, Y. F.; Hou, J. H. *Adv. Mater.* **2012**, *24*, 3383−3389.
(46) Rose, A. *Phys. Rev.* **1955**, *97*, 1538−1544.
(47) Diaz de Zerio Mendaza, A.; Bergqvist, J.; Backe, O.; Lindqvist, C.; Kroon, R.; Gao, F.; Andersson, M. R.; Olsson, E.; Inganas, O.; Muller, C. *J. Mater. Chem. A* **2014**, *2*, 14354−14359.
(48) Ye, L.; Zhou, C.; Meng, H.; Wu, H.-H.; Lin, C.-C.; Liao, H.-H.; Zhang, S.; Hou, J. *J. Mater. Chem. C* **2015**, *3*, 564−569.
(49) Ye, L.; Jing, Y.; Guo, X.; Sun, H.; Zhang, S.; Zhang, M.; Huo, L.; Hou, J. *J. Phys. Chem. C* **2013**, *117*, 14920−14928.

DOI: 10.1021/acs.macromol.5b00649
Macromolecules 2015, 48, 3493−3499